Dose-Response:
An International Journal
July-September 2019:1-11

DOI: 10.1177/1559325819869502
journals.sagepub.com/home/dos
SAGE

Novel Route of Synthesis of PCL-CuONPs Composites With Antimicrobial Properties

Antonio Muñoz-Escobar[1], Álvaro de Jesús Ruíz-Baltazar[2], and Simón Yobanny Reyes-López[1]

Abstract

Nanoparticles of metals can be toxic to bacteria, showing biocidal activities at low concentrations. Metal, oxide, or compounds based on copper are applied like antimicrobial agents. The capacity of integration of metallic nanoparticles in polymer matrices has improved the antimicrobial behavior, resulting in the search for composites with increased bactericidal properties. A polycaprolactone (PCL) film polymer with copper oxide nanoparticles (CuONPs) was prepared. Dynamic light scattering analysis showed the sizes from 88 to 97 nm of CuONPs. Scanning electron microscopy (SEM) revealed CuONPs with semispherical shapes with diameter 35 nm. The prepared PCL-CuONPs exhibited a nanoporous structure by SEM. The antibacterial applicability of the composite was evaluated to determine the minimum inhibitory concentration in 6 different bacteria and the experimental tests were carried by disk diffusion and spectrophotometric methods. The PCL-CuONPs exhibit a considerable antibacterial effect in gram-positive bacteria in contrast to gram-negative bacteria. The preparation of PCL-CuONPs was simple, fast, and low cost for practical application as wound dressings.

Keywords

nanofibers, composites, PCL, copper oxide nanoparticles, antibacterial activity

Introduction

The fast emergence of antibiotic-resistant bacteria is occurring on a world scale. Several decades after the first clinical use of antibiotics, bacterial infections have again become a threat. The overuse and misuse of these medications as well as a lack of new antibacterial materials have been the cause of this antibiotic resistance crisis. The Centers for Disease Control and Prevention has classified several bacteria as presenting urgent, serious, and concerning threats, many of which are *Staphylococcus* spp., *Streptococcus* spp., and *Pseudomonas* spp.[1] and also Enterobacteria such as *Escherichia coli* and *Klebsiella* species, which have shown important antibiotic resistance effects, producing serious intestinal, skin, and other soft tissue infections.[2]

The emergence of nanotechnology has provided a solid platform for adjusting the physicochemical properties of numerous materials to generate an alternative to antibiotics to control bacterial infections.[3] Nanomaterials, such as nanoparticles, provide higher surface area to volume ratio with lower usage of materials leading to be more effective in most applications.[4] The synthesis of nanoparticles can be done through several methods, such as physical, chemical, and biological. With the exception of the last one, they can offer high production rate and better size control of the nanoparticles, but they can be expensive due to high-energy and capital requirements.[5] Chemical reduction method is preferred, because this method is easy, cost-effective, and efficient, and it can control the size and size dispersion by optimizing the experimental factors.[6] Most of the chemical reduction methods are done in an aqueous medium, thus limiting the coupling of the synthesized nanoparticles only on hydrophilic polymers.

Among all nanoparticles, metal oxide nanoparticles offer promise as antimicrobial agents against a broad spectrum of

[1] Instituto de Ciencias Biomédicas, Universidad Autónoma de Ciudad Juárez, Envolvente del PRONAF y Estocolmo s/n, Ciudad Juárez, Chihuahua, Mexico
[2] Conacyt-Centro de Física Aplicada y Tecnología Avanzada, Universidad Nacional Autónoma de México, Juriquilla Querétaro, Mexico

Received 24 January 2019; received revised 15 July 2019; accepted 18 July 2019

Corresponding Author:
Simón Yobanny Reyes-López, Instituto de Ciencias Biomédicas, Universidad Autónoma de Ciudad Juárez, Envolvente del PRONAF y Estocolmo s/n, Ciudad Juárez, Chihuahua 32300, Mexico.
Email: simon.reyes@uacj.mx

microorganisms, including multidrug-resistant strains of both gram-positive and gram-negative microbes.[7] Copper oxide nanoparticles (CuONPs) stand out by being widely used in conductor, electrical, and optical fields and also possess very well-known antibacterial properties.[8] They were effective in killing a wide range of bacterial pathogens involved in nosocomial infections.[9] They are also a powerful biocide toward fungi[10] and various types of algae,[11] and they present antiviral capabilities.[9] Their antimicrobial activity relies on the ability to release metallic ions and the extent of their surface area.[12] Cu^{2+} ions released from CuONPs generate damage to proteins and lipids of the cell membrane, due to the fact that they are negatively charged. Additionally, Cu^{2+} ions possess high redox properties, which produce reactive oxygen species, producing alterations in subcellular components, including damage to DNA double-helix molecule.[13]

Metal oxide/polymer composites can be synthesized by an efficient fabrication process, namely, electrospinning.[14,15] The electrospinning technique has become popular in recent years due to its simplicity and versatile process. The fibers capable of being electrospun have diameters as small as below a hundred nanometers. Electrospinning utilizes an electric field strong enough to overcome the surface tension of a polymeric solution producing a spinning jet, leading to deposition of the fibers on a collector.[16]

The selected polymer is one of the primarily factors for the successful preparation of antimicrobial nanofibers.[15] Polycaprolactone (PCL) is an electrospinnable, hydrophobic, and semicrystalline polymer that has been considered for biomedical applications. It can be used as a long-term implant delivery device, thanks to its short in vivo degradation rate and high drug permeability.[17] Polycaprolactone has also been used for skin regeneration applications, scaffolds for fibroblasts support, nanocomposites for bone repair, ureteral substitution, and lately electrospun composite nanofibers.[18]

Polymer–metal nanoparticles composites appear to extend the applications of biocide metals. The antibacterial properties of CuONPs can work together with the function of a polymer film as a wound dressing to protect from contamination and temporarily compensate for damaged skin. The aim of this contribution is to develop an inexpensive, effective, and nonaqueous procedure for synthesis of CuONPs to functionalize polymeric PCL nanofibers and assess their antibacterial performance on several microorganisms of clinical importance.

Materials and Methods

Materials

All the chemicals used were of analytical grade and purchased from Sigma-Aldrich: copper nitrate ($Cu(NO_3)_2$), poly ε-caprolactone with an average molecular weight of 80 000, N, gallic acid (≥97.5%), dimethylformamide (DMF; ≥98.5), and tetrahydrofuran (THF; ≥99.5%). All chemical reagents were used as received. Muüller-Hinton broth and agar plates were used for antibacterial test. *Escherichia coli* (ATCC25922), *Streptococcus mutans* (ATCC25175), *Klebsiella oxytoca* (ATCC13182), *Staphylococcus aureus* (ATCC25923), *Pseudomonas aeruginosa* (ATCC27853), and *Bacillus subtilis* (ATCC19163) microorganisms were obtained from American Type Culture Collection.

Copper Oxide Nanoparticles Preparation

The synthesis of CuONPs was carried out in a nonaqueous solution with ratio of 7:3 of DMF and THF, respectively; then copper nitrate was added as a precursor agent into this solution.[2,18] The solution was placed under magnetic stirring, and gallic acid (0.02 M) in DMF and THF solution was added dropwise at a drop per minute rate until a color change to dark green was observed. Particle size was controlled by the initial concentrations of copper nitrate (0, 25, 50, 100, and 200 mM), according to previous studies.[2,18] UV–vis absorption spectra were measured at room temperature in a Cary100 spectrophotometer (Varian Corp) with a variable wavelength between 100 and 900 nm using a 10-mm quartz cell. Particle size and distribution were measured by dynamic light scattering in an HORIBA SZ-100 Nanoparticle Analyzer (HORIBA, Ltd., USA). WITec's Raman spectrophotometer alpha300R, with a 532-nm laser, was used for Raman imaging. X-ray diffraction crystallographic study was carried out using XPERT PRO PANalytical diffractometer (PANalytical, The Netherlands), in the scanning range of 2θ from 20° to 80° (CuKα1; 35 kV; 25 mA). Finally, the morphologies of the CuONPs and fibers collected on carbon-coated copper grids were observed with a scanning electron microscopy (SEM, JEOLJSM-6400, (JEOL, Japan)) operated at 20 kV, equipped with energy dispersive Xx-ray spectroscopy (EDS). Fourier-transform infrared spectroscopy spectra were taken with an Alpha Platinum-ATR spectrometer. Thermal evolution of the fibers was determined by thermogravimetric analysis and differential thermal analysis (DTA) using a SDT Q600 V20.9 Build 20 instrument (TA Co. LTD., USA). X-ray diffraction was employed to identify crystalline phases present in fiber samples treated at 800°C and 1600°C. An instrument X'Pert PRO PANalytical was used, with Cu kα = 1.54056, 20 kV, 10° to 80°, by the powder method, and a 2°/min scanning speed.

Preparation and Fabrication of Nanofibers Composites

The second step was the preparation of nanofibers by electrospinning; the simple method consisted in forming a viscous solution of PCL 10% (m/v) with the newly prepared CuONPs solutions under magnetic stirring at room temperature (see Figure 1). The resulting viscous solution of PCL with copper nanoparticles was loaded into a syringe connected to a stainless-steel needle of 1.25-mm inner diameter. The steel needle was connected to a high-voltage generator, and an aluminum foil served as the counter electrode. A dense web of fibers was collected on the aluminum foil. The used electrical potential amounted to 15 kV, the distance between the capillary and the substrate electrode was 10 cm, and the feeding rate of

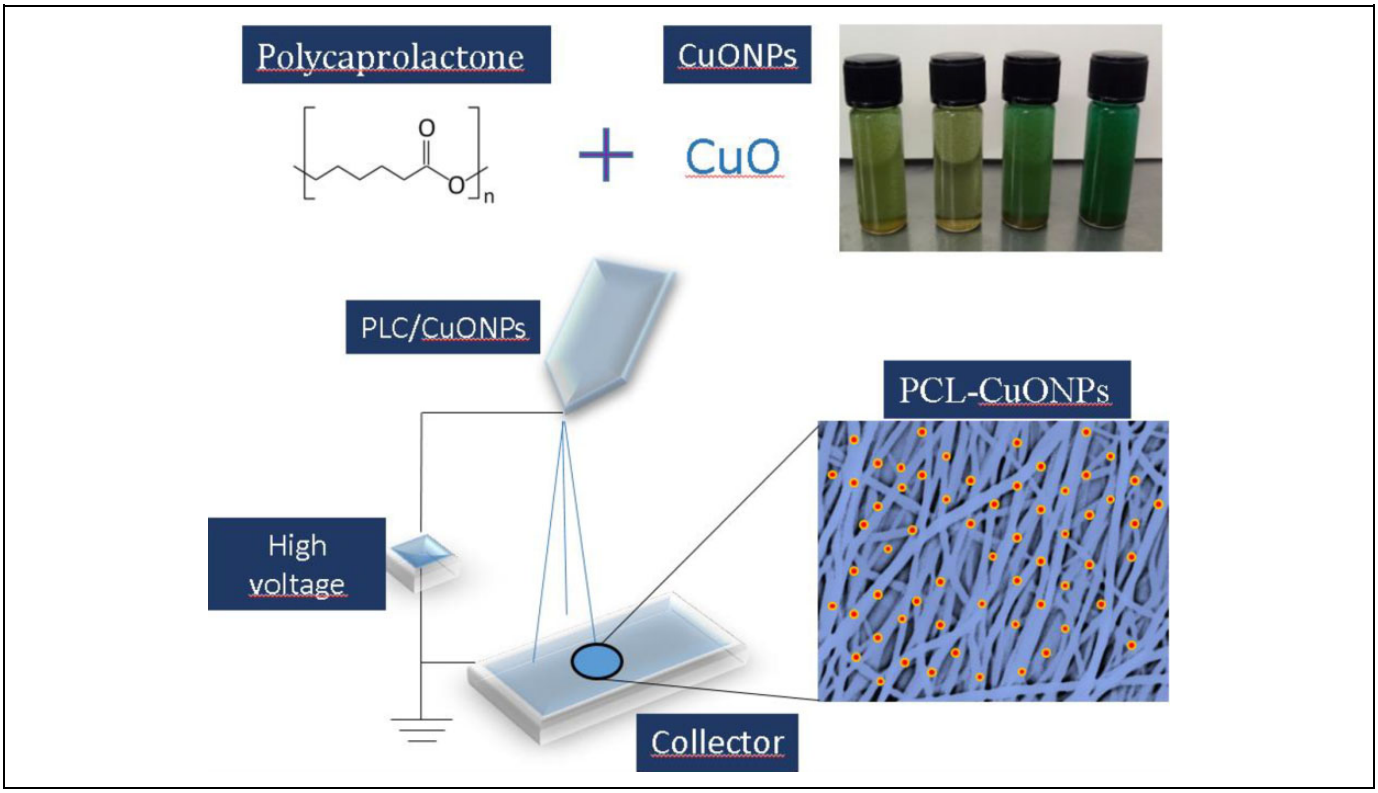

Figure 1. Schematic representation of the synthesis of PCL-CuONPs composites. PCL-CuONPs indicates polycaprolactone with copper oxide nanoparticles.

the solution in syringe pump was 15 to 20 μL/min. The electrospinning assay was performed at 25°C.

Antibacterial Activity

Disk-diffusion method was performed to PCL-CuONPs nanocomposites to measure its antibacterial activity. The microbial species, *E coli*, *S mutans*, *K oxytoca*, *S aureus*, *P aeruginosa*, and *B subtilis*, were cultured in Muüller-Hinton broth for 20 hours at 37°C before the test. According to the McFarland scale (1.3×10^6 CFU/mL), 100 μL of standardized suspensions of each bacterium was placed on Muüller-Hinton agar plates. Samples of PCL-CuONPs (1 cm × 1 cm) were cut in circular discs and submitted to the inhibition zone tests. The sterilized disks were then positioned on the 6 different microbial species culture plates, being incubated for 24 hours at 37°C. The antibacterial effect was determined by the measurement of clear zones resultant to inhibition formed around the disks. All tests for each microorganism were made in triplicate.

Minimum inhibitory concentration (MIC) was determined using the microbroth dilution method in a microplate reader Multiskan MCC Fisher Scientific (USA). In the microplate wells, one PCL-CuONPs disc of the corresponding concentrations of 0, 25, 50, 100, and 200 mM was placed for each bacteria. The microplate was incubated at 37°C for 12 hours. The turbidity of the media was observed at various time intervals at 570 nm using a UV spectrophotometer. After that time, the final absorbance was measured to estimate the inhibition percentage. The antimicrobial test for all microorganisms and nanofibers was made in triplicate. All data were analyzed by IBM SPSS Statistics 25 and are expressed as mean values ± standard error. Statistical analyses were carried out using analysis of variance and Tukey multiple comparison test. A P value $\leq .05$ was considered statistically significant.

Results and Discussions

Initial formation of CuONPs was visualized from color changes in the solutions, from blue green to dark green, which correspond to the formation of CuONPs, as shown in Figure 2A.[19] UV–vis analysis exhibited well-defined plasmon band absorption for CuONPs (Figure 2B). The study performed by Varughese et al depicts the optical absorption spectrum of CuONPs, displaying an excitonic absorption peak at 280 nm, which is attributed to the formation of cupric oxide nanoparticles.[20] Our study shows the absorption peaks from 270 to 285 nm increasing according to the precursor salt concentration, as reported previously. The observed changes in the spectrum reflect the characteristic pattern of CuONPs formation by reducing copper ions with gallic acid present in reductive solution of DMF and THF.

The size and shape of the resultant particles were elucidated with SEM (Figures 2B and 3A). The obtained nanoparticles observed from the micrograph majority were mostly spherical

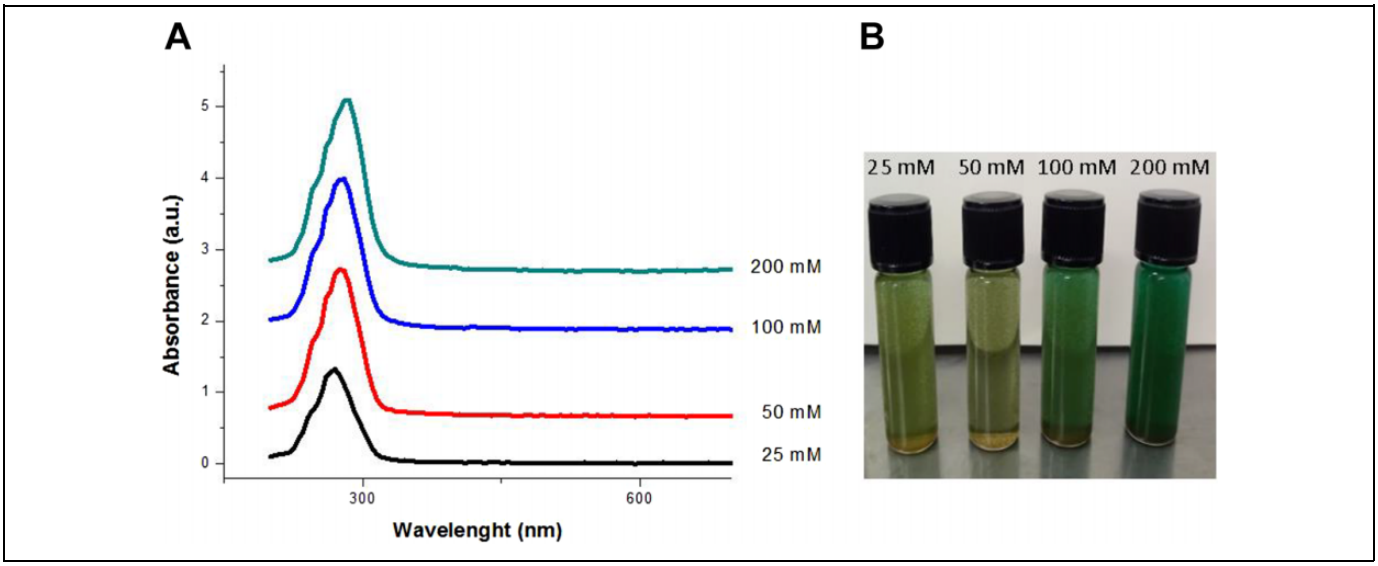

Figure 2. UV–vis spectra of CuONPs (A) and the change of color of each solution (B). CuONPs indicates copper oxide nanoparticles; UV, ultraviolet.

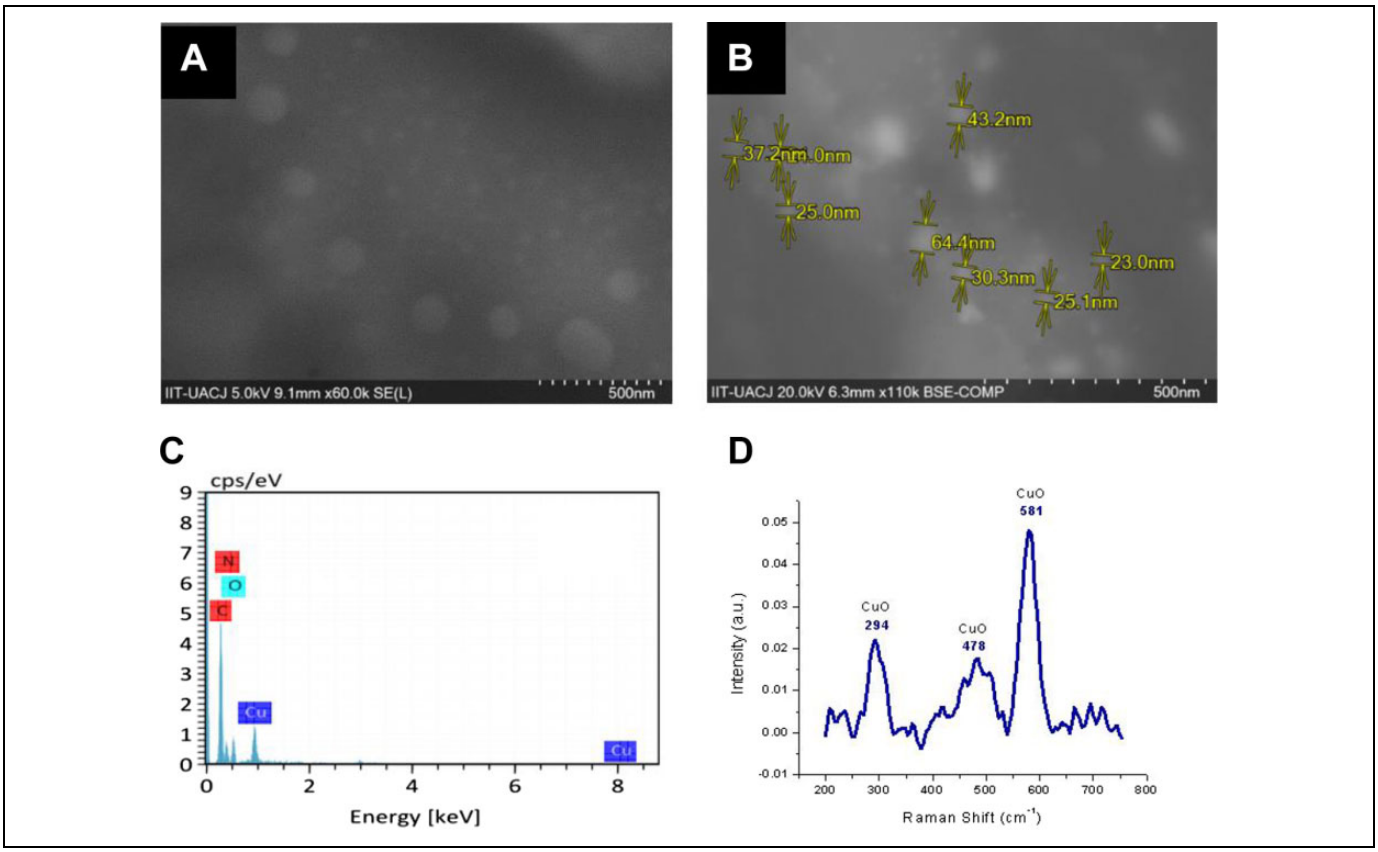

Figure 3. The SEM images of CuONPs (A and B), EDS spectra (C), and Raman spectra (D). CuONPs indicates copper oxide nanoparticles; EDS, energy dispersive x-ray spectroscopy; SEM, scanning electron microscopy.

and some of them were agglomerated. Without any protecting agents, the general expectation would be that the nanoparticles would tend to agglomerate even more and that the particle sizes would be larger and more variable. However, there was noted only some variation in nanoparticle size. Most sizes of the particles ranged from 20 to 45 nm, and the average size was estimated at 35 nm for all concentrations, according to the size distribution shown in Figure 4. Nanoparticle sizes were not

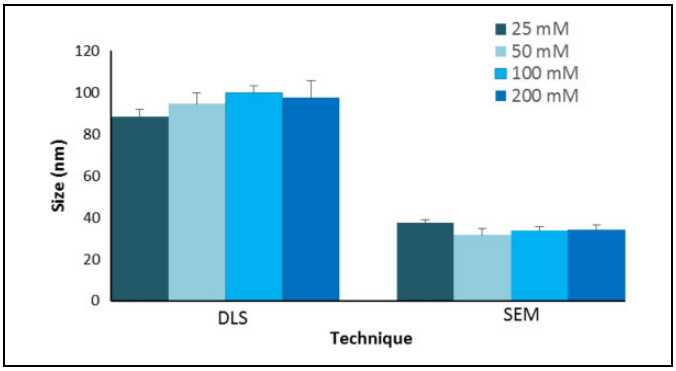

Figure 4. Size measurements of CuONPs obtained by DLS analysis and SEM micrographs. CuONPs indicates copper oxide nanoparticles; DLS, dynamic light scattering; SEM, scanning electron microscopy

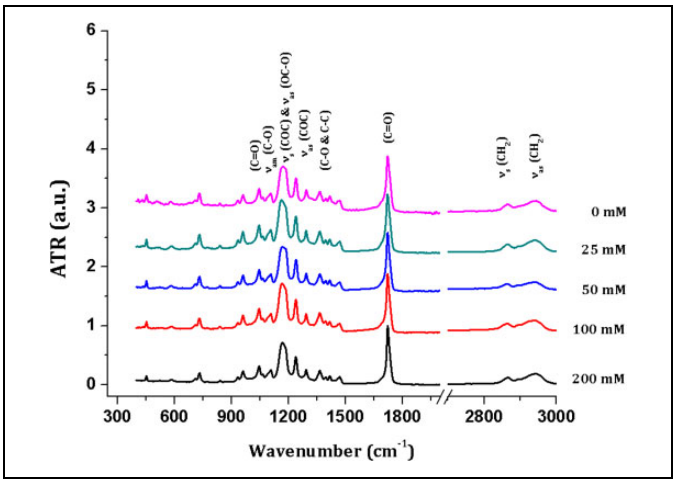

Figure 5. Infrared spectra of electrospun PCL and PCL-CuONPs fibers. PCL-CuONPs indicates polycaprolactone with copper oxide nanoparticles.

directly proportional to the precursor salt concentration. The hydrodynamic diameters of CuONPs were assessed, founding that the cumulant diameters of CuONPs had sizes from 88 to 97 nm (Figure 4). This could be explained by the agglomerations of CuONPs observed previously by SEM. On the other hand, the initial amounts of copper nitrate and reducing agents left no residue and the reaction was assumed to be complete. It can be concluded that Cu ions can be reduced to CuO at room temperature with this methodology and don't require a longer period than other techniques. The elemental analysis (EDS) was performed to prove the presence of copper component in the prepared sample particles. Figure 3C shows the spectrum of CuONPs obtained by elemental microprobe EDS analysis. The results show that carbon, oxygen, nitrogen, and copper are the principal elements forming the sample. Further evidence for the synthesis of CuONPs is provided by the Raman spectra of the synthesized nanoparticles illustrated in Figure 3D. Raman spectra provide information about the nature of the CuONPs, which is essential for verifying the purity of the oxide. It can be seen that there are 3 Raman peaks in the sample, at 294 cm^{-1}, 581 cm^{-1}, and a very broad band from 400 to 600 cm^{-1}, which are characteristics bands for CuO. It was possible to discard the Cu_2O presence in the films, due to spectra for Cu_2O showing very different features at distinct bands at 150, 220, and 625 cm^{-1}.[21] X-ray diffraction was employed to characterize the crystal structure and phase purity of the nanoparticles. X-ray diffraction patterns of the CuONPs exhibit a crystalline structure of single-phase monoclinic CuO according to JCPDS file No. 45-0937. The not formation of peaks related to another single-phase of Cu_xO_y was confirmed by the absence of Cu_2O_3, Cu_2O, and Cu planes, in agreement with Raman spectra.

Infrared spectra of electrospun PCL and PCL-CuONPs 25, 50, 100, and 200 mM fibers are shown in Figure 5. They all exhibited the absorption bands of the functional groups of the polymer including both absorption bands at 1719 and 2945 cm^{-1} corresponding to the functional groups C=O and C–H, respectively. There was no shift in peak positions of the CuONPs-loaded PCL fibers compared to plain PCL films.

Thermogravimetric analysis is used to analyze the decomposition temperature of PCL and its different CuONPs

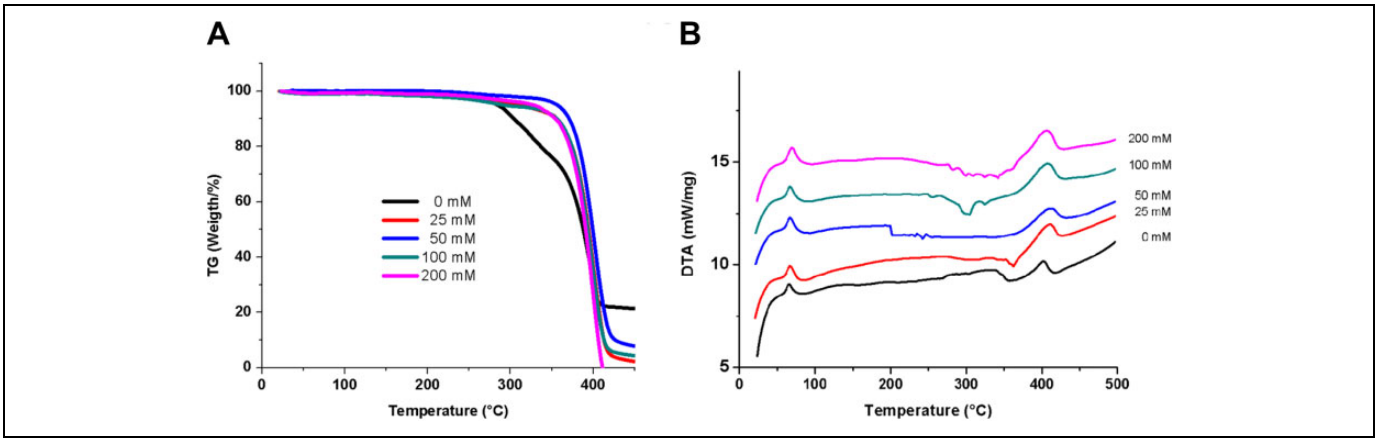

Figure 6. The TGA (A) and DTA (B) of PCL and PCL-CuONPs fibers. DTA indicates differential thermal analysis; PCL-CuONPs, polycaprolactone with copper oxide nanoparticles; TGA, thermogravimetric analysis.

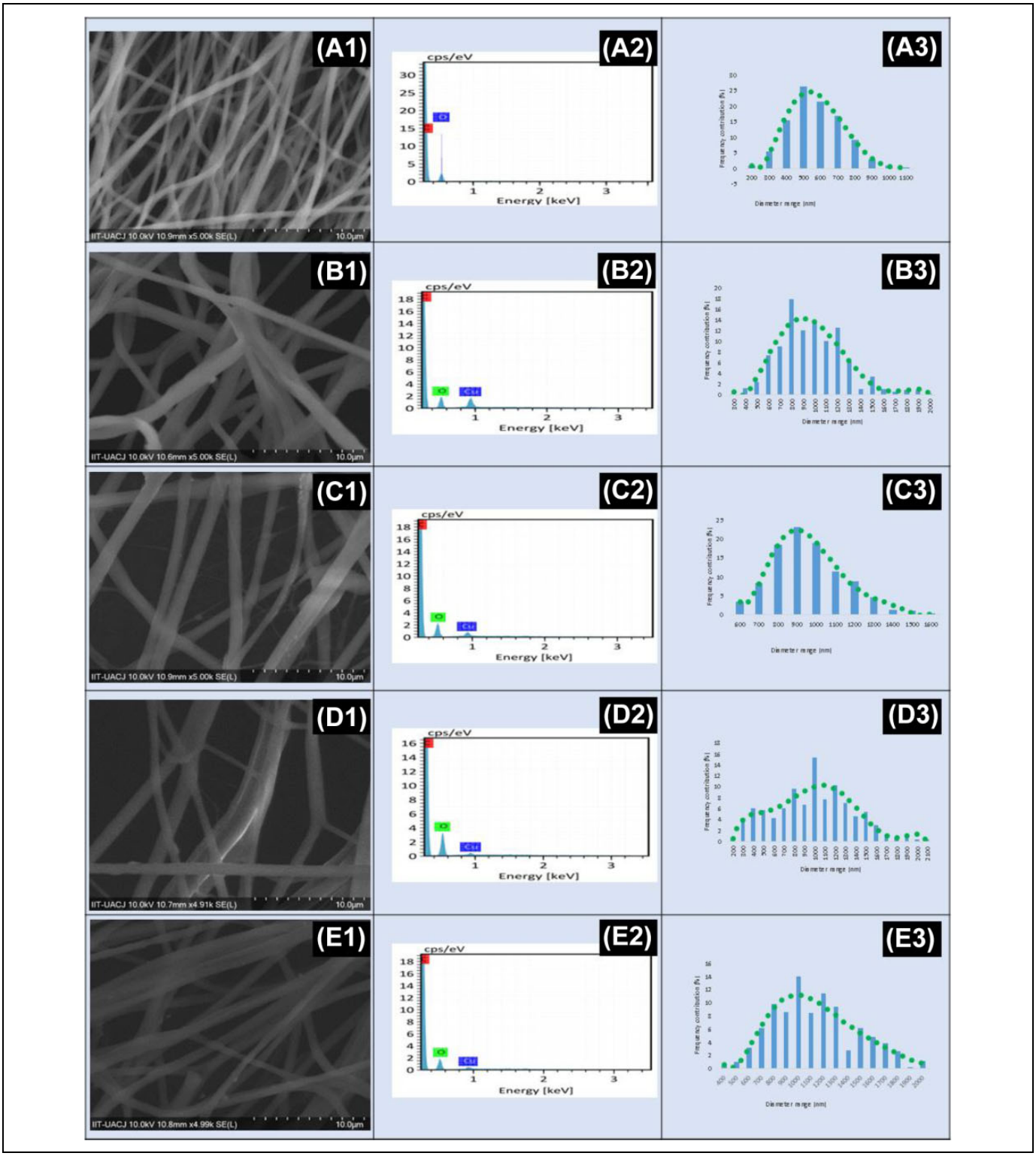

Figure 7. The SEM images of PCL-CuONPs 0 mM (A1), 25 mM (B1), 50 mM (C1), 100 mM (D1), and 200 mM (E1), their respective EDS spectra (A2-E2), and their histogram distribution (a3-e3). EDS indicates energy dispersive X-ray spectroscopy; PCL-CuONPs, polycaprolactone with copper oxide nanoparticles; SEM, scanning electron microscopy.

composites and the weight change (%) with respect to temperature (°C). From the graph exhibited in Figure 6, it showed that PCL thermal degradation begins at 280°C in a single stage, which is related to the complete process which includes the dehydration of the saccharide rings, according to Noor and Ansari.[22] Weight loss of PCL-CuONPs composites was also

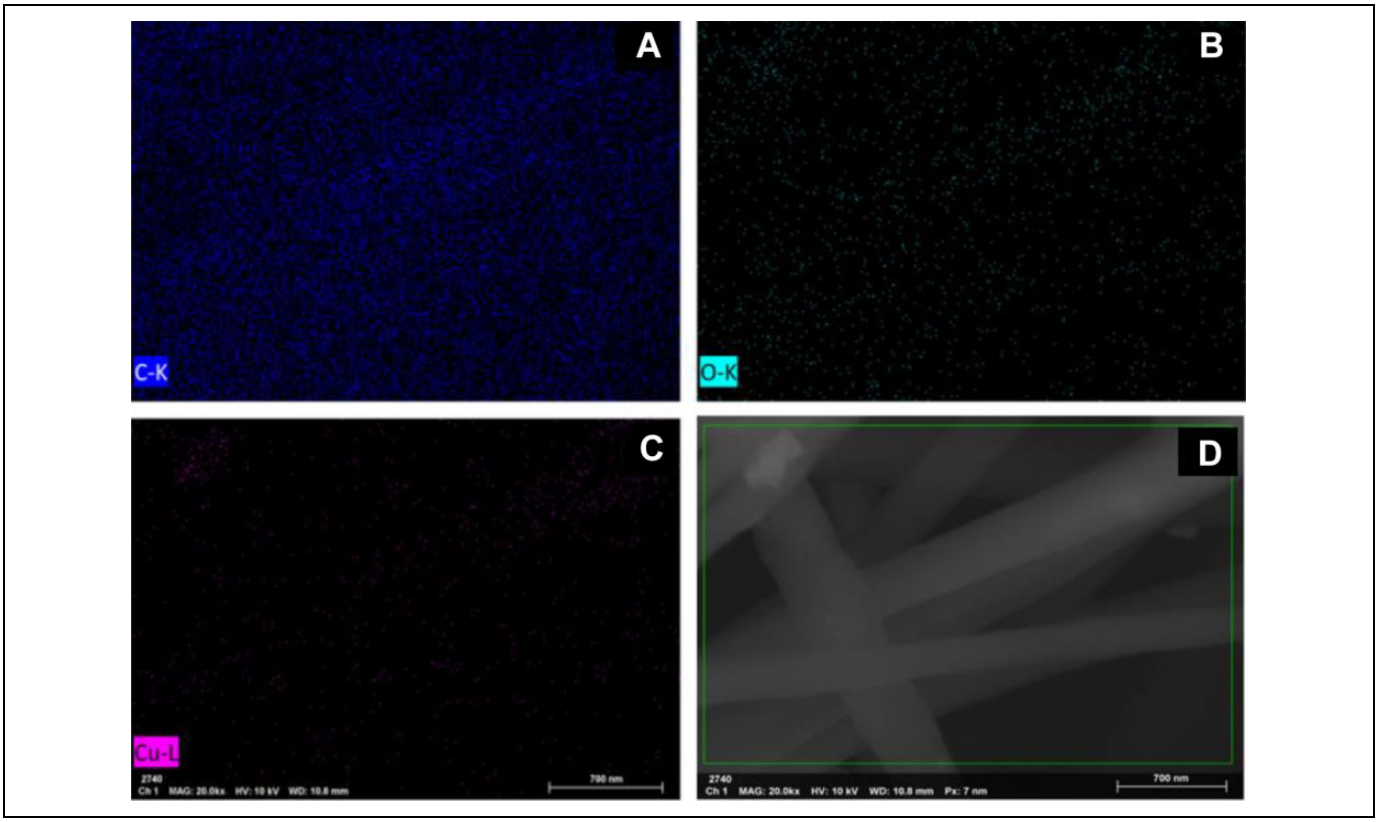

Figure 8. The EDS mapping showing distribution of carbon (A), oxygen (B), and copper ions (C) in the polymer membrane of PCL-CuONPs 200 mM displayed in the SEM image (D). EDS indicates energy dispersive X-ray spectroscopy; PCL-CuONPs, polycaprolactone with copper oxide nanoparticles; SEM, scanning electron microscopy.

verified. The curves show a shift to a higher temperature for PCL-CuONPs because of the copper oxide presence. It means that PCL-CuONPs exhibit a better thermal stability compared to pure PCL. The fibers were further characterized by DTA, showing an endothermic melting peak at about 66°C, an endothermic decomposition peak at about 360°C, and an exothermic peak at about 413°C. These 3 observed phenomena clearly identify PCL composite fibers.

Scanning electron microscopy images in Figure 7 show that the obtained fibers present a cylindrical smooth surface and free area of beads, precipitates, and fractures. It is evident from the SEM images of PCL-CuONPs nanofibers scaffolds that the electrospun nanofibers were smooth and uniform with optimized electrospinning parameters. The average diameters of PCL and PCL-CuONPs nanofibers were from 522 $\pm$ 156, 925 $\pm$ 279, 908 $\pm$ 18, 945 $\pm$ 388, and 1082 $\pm$ 329 nm for CuONPs contents of 0, 1, 10, 50, and 100 nM, respectively. The diameters of these nanofibers were observed to increase upon an increase in the content of the CuONPs. Results obtained by electron microscopy showed the existing relation between size distribution and concentration of CuO nanoparticles. The presence of CuONPs in the solution increased the electrical charge and conductivity, which resulted in a wider diameter of the fibers. Energy dispersive X-ray spectroscopy mapping was used to characterize the distribution of Cu^{2+} in the PCL composite membrane, due to the distribution of nanoparticles in PCL fibers directly influences the antimicrobial performance of the membrane. The homogeneous distribution of elements C, O, and Cu in EDS mapping indicated that the CuONPs nanoparticles were homogeneously distributed.

Figure 8 shows the SEM and EDS maps at 20 000× that further proves the presence of Cu in the PCL fibers at 200 mM. CuO nanoparticles were found in the surface and into the fibers. The blue and light blue maps for carbon and oxygen EDS maps in Figure 8A and B give the same skeleton of the fibers. The magenta dots on the EDS map in Figure 8C, which stand for the detected copper, clearly covered the fiber.

In order to examine whether the nanocomposite of PCL with in situ generated CuONPs possess antibacterial activity, the disk diffusion method was performed and listed in Table 1. Several articles have already demonstrated an excellent antimicrobial activity of CuONPs against a wide range of bacteria. However, the concentrations reported have been high, such as the case for *E coli* in which 0.02 g and 0.75 mg were used.[23,24] In the antimicrobial tests, CuONPs weren't used directly due to the fact that equivalent concentration would be very low and difficult to manipulate. For example, the concentration of 200 mM CuONPs would have an equivalent of 0.32 mg and besides that a composite allows the controlled release of Cu

Table 1. Inhibition Halo Test Results for Each Bacteria at Different Concentrations.

Concentration (mM)	Halo Size (mm)	Concentration (mM)	Halo Size (mm)
Gram-Negative Bacteria		Gram-Positive Bacteria	
Escherichia coli		*Bacillus subtilis*	
25	–	25	–
50	–	50	–
100	–	100	–
200	–	200	–
Pseudomonas aeruginosa		*Staphylococcus aureus*	
25	7.00	25	
50	7.49	50	–
100	7.86	100	–
200	11.20	200	6.79
Klebsiella oxytoca		*Streptococcus mutans*	
25	–	25	–
50	–	50	–
100	–	100	–
200	6.69	200	–

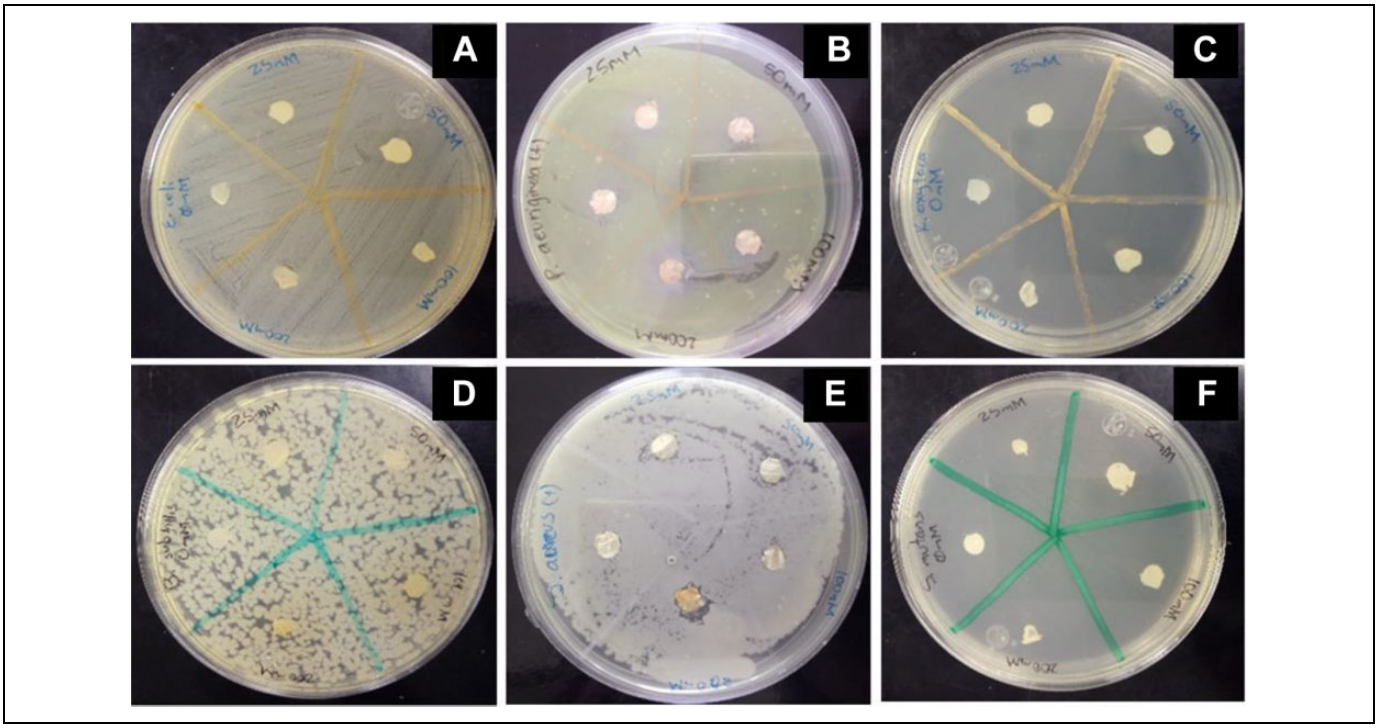

Figure 9. Images of zones of inhibition against (A) *Escherichia coli*, (B) *Pseudomonas aeruginosa*, (C) *Klebsiella oxytoca*, (D) *Bacillus subtilis*, (E) *Staphylococcus aureus*, and (F) *Streptococcus mutans*.

ions. Maximum zone of inhibition of pathogenic microorganisms, 3 gram-positive and 3 gram-negative bacteria, was measured, showing the best inhibition results of PCL-CuONPs nanofiber scaffolds against the gram-negative bacteria *P aeruginosa* showing effectiveness since the smallest concentration of CuONPs, continuing its effect along the concentrations of 50 and 100 mM, and being significantly increased at 200 mM. *Klebsiella oxytoca* and *S aureus* only showed a small inhibition zone in the greatest concentration of CuONPs. Inhibition halo in the other tested bacteria wasn't observable in any PCL-CuONPs concentration. It has been demonstrated that the antibacterial response of composites containing metallic elements, such as copper, depends on the concentration of metal ions according to Figure 9 and Table 1, as well as dissolution of metals released in growth media for both gram-positive and gram-negative bacteria.[25]

In the interest of verifying if the dissolution of the Cu^{2+} would increase in a liquid media, and therefore increase its antibacterial properties, we proceed to perform the optical density method. Figure 10 shows results of the inhibition

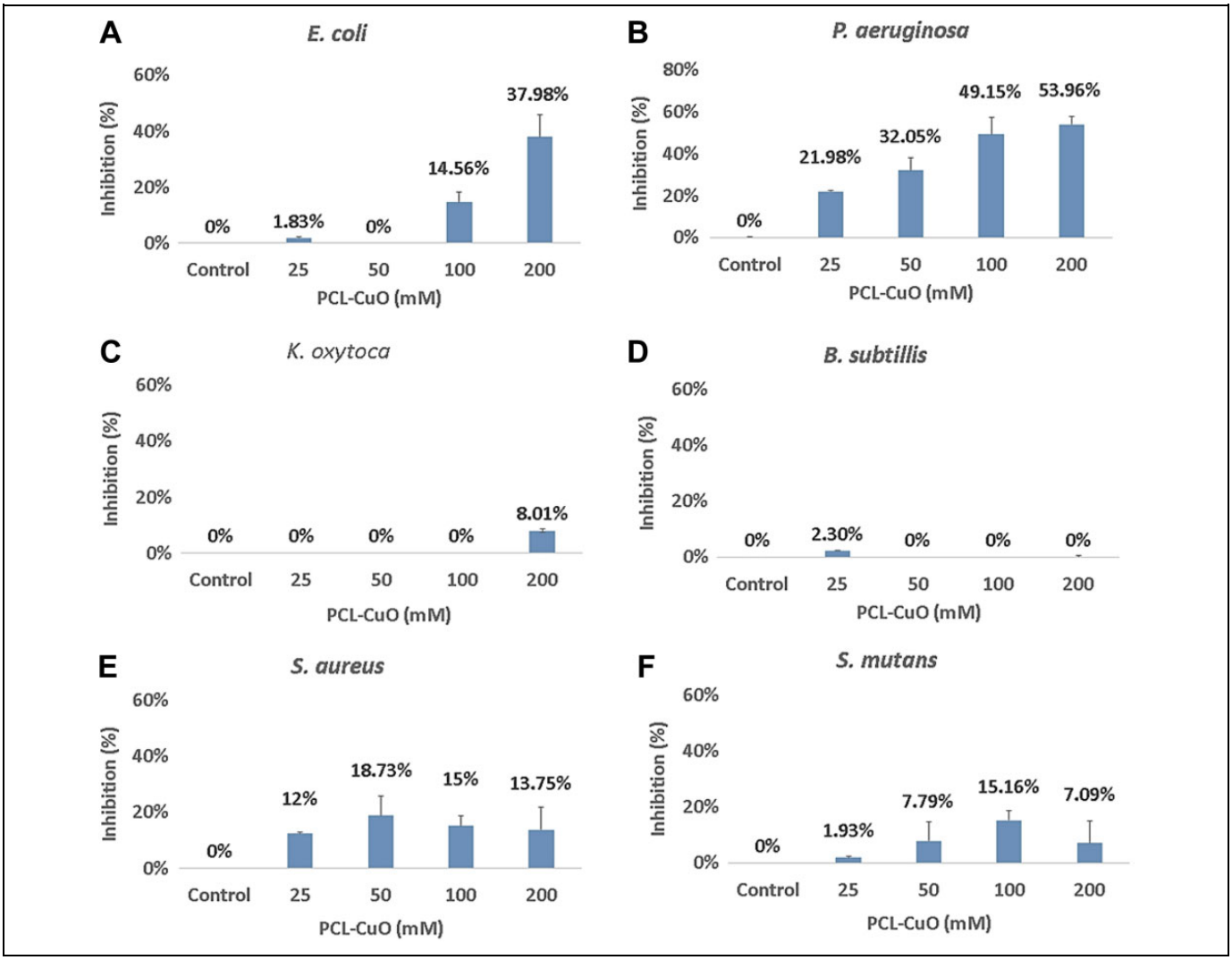

Figure 10. Inhibition effect of PCL-CuONPs against (A) *Escherichia coli*, (B) *Pseudomonas aeruginosa*, (C) *Klebsiella oxytoca*, (D) *Bacillus subtilis*, (E) *Staphylococcus aureus*, and (F) *Streptococcus mutans.* PCL-CuONPs indicates polycaprolactone with copper oxide nanoparticles.

percentage of each bacteria, which were equal in *K oxytoca* and *P aeruginosa* as those obtained in disk diffusion method, showing again only a small inhibition of *K oxytoca* in the biggest concentration, and demonstrating again the MIC of 25 mM of PCL-CuONPs in *P aeruginosa*. *Escherichia coli* presented a 14.56% of inhibition at PCL-CuONPs 100 mM, which increased more than 2-fold to 37.98% in 200mM. Gram-positive bacteria displayed slightly inhibition results for *S aureus* being equal for all the concentrations, beginning from 12% and also for *S mutans*, which inhibition started from the smallest concentration from 1.93% and increased and maintained to 7.79%. *Bacillus subtilis* had no inhibitory effect even at high CuONPs concentration. The turbidity of the media was observed at various time intervals in order to register changes in bacteria growth rate. Only 2 gram-negative bacteria had significant differences compared to the control, *E coli*, which growth velocity decreased at the highest concentration of copper and *P aeruginosa* which growth rate started to fluctuate from 100 mM and was clearly affected at 200 mM.

In our present study, both gram-positive and gram-negative bacteria were used to assess the antibacterial properties and the results indicated that PCL-CuONPs did not exhibit a strong antibacterial effect in gram-positive bacteria in contrast to gram-negative bacteria. Gram-negative bacteria present a cell wall composed of a cytoplasmic membrane, a thin peptidoglycan layer, and an additional outer membrane containing lipopolysaccharide, which face the external environment. The scarce width of the cell wall increases the vulnerability of these bacteria to copper ions released by the nanoparticles on the polymer. *Pseudomonas aeruginosa*, the gram-negative and the main pathogenic bacteria of nosocomial infections, was used to investigate the antimicrobial activity of our PCL-CuONPs membranes. After exposure of the composite fibers in the bacterial suspension, the inhibition growth of *P aeruginosa* was observed by turbidimetry. The results demonstrated that the

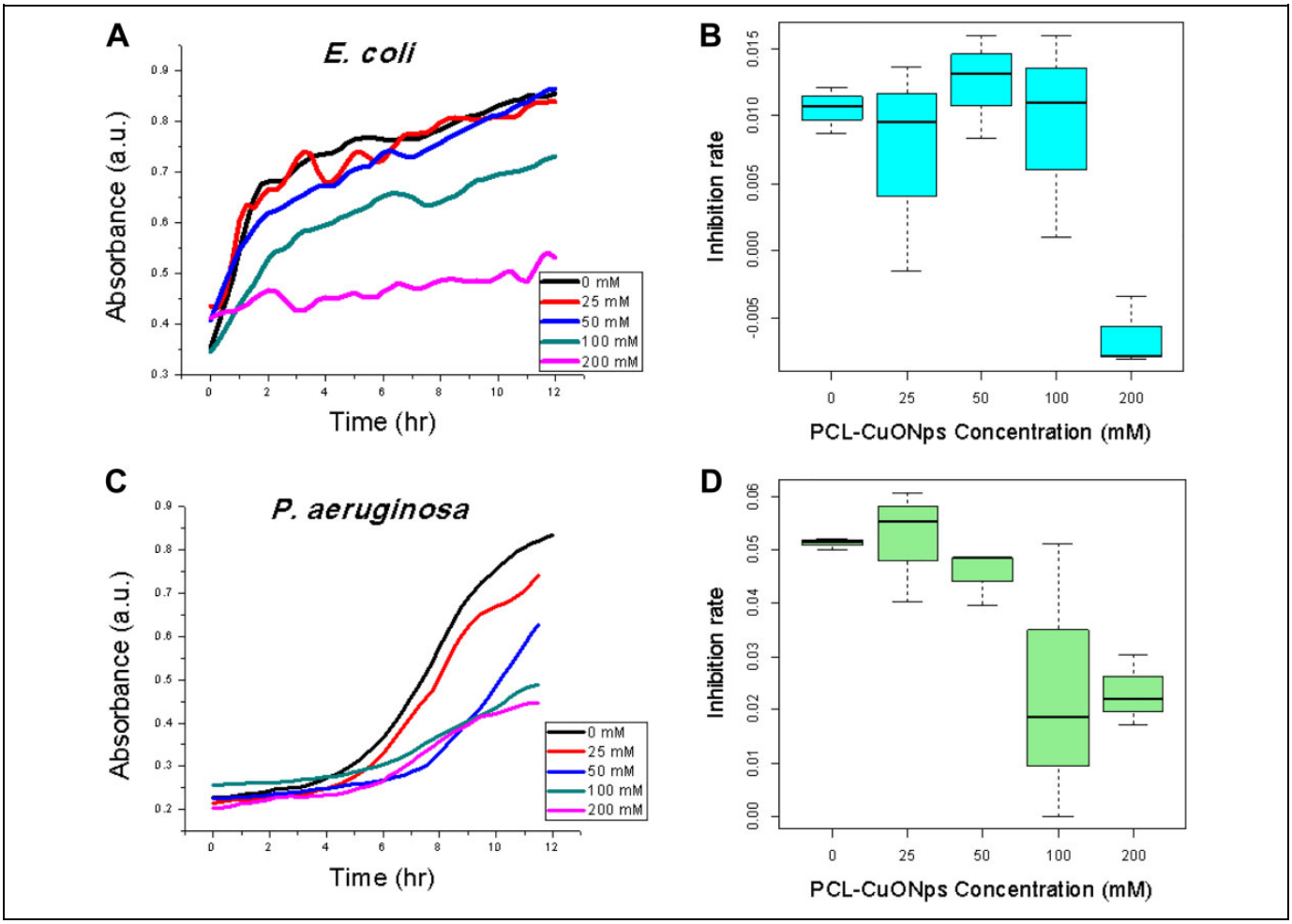

Figure 11. Comparative growth curve of (A) *Escherichia coli* and (C) *Pseudomonas aeruginosa* and their respective box plot charts (B and D) indicating the differences in growth rate after being exposed to different concentrations for PCL-CuONPs. PCL-CuONPs indicates polycaprolactone with copper oxide nanoparticles.

prepared membranes with CuONPs had the strongest antibacterial effect against these pathogenic bacteria, which would significantly reduce the risk of postoperative infections.

Microorganisms develop drug resistance by various mechanisms, the new advances in nanocomposites given the opportunity to be an alternative to diseases caused by drug-resistant microorganisms. The expansion of technology for the synthesis of nanocomposites has also transformed the field of nanomedicine. The synthesis of NPs by easy methods reduces the environmental damage related to chemical synthesis (Figure 11).

Conclusion

Polycaprolactone with CuONPs fibers with diameters ranging from 925 to 1080 nm were successfully obtained by electrospinning technique. Orientation, morphology, and diameter were influenced by the increment on CuONPs concentration, with the smaller diameter present in samples prepared from low concentrated solutions. Bacterial growth was not affected by pure PCL fibers; however, the presence and concentration of CuONPs determined gradually the antimicrobial activity on bacteria, such as *P aeruginosa*, which the MIC was displayed at 25 mM. Also, gram-negative bacteria demonstrated to be more sensitive to PCL-CuONPs composites than gram-positive strains, determining a dose-dependent activity. The PCL-CuONPs composites obtained by electrospinning technique demonstrated to have a high potential for biomedical applications. The composites provided an alternative for the treatment of many diseases that are difficult to treat by present-day methodology.

Acknowledgments

Thanks to PRODEP, Universidad Autónoma de Ciudad Juárez and CONACYT for supporting this investigation.

Declaration of Conflicting Interests

The author(s) declared no potential conflicts of interest with respect to the research, authorship, and/or publication of this article.

Funding

The author(s) disclosed receipt of the following financial support for the research, authorship, and/or publication of this article: PRODEP, Universidad Autónoma de Ciudad Juárez, and CONACYT.

ORCID iD

Simón Yobanny Reyes-López https://orcid.org/0000-0002-9017-3233

References

1. Ventola CL. The antibiotic resistance crisis. Part 1: causes and threats. *P T*. 2015;40(4): 277-283.
2. Pazos-Ortiz E, Roque-Ruiz JH, Hinójos-Márquez EA, et al. Dose-dependent antimicrobial activity of silver nanoparticles on polycaprolactone fibers against gram-positive and gram-negative bacteria. *J Nanomater*. 2017;2017(4752314):1-9.
3. Beyth N, Houri-Haddad Y, Domb A, Khan W, Hazan R.Alternative antimicrobial approach: nano-antimicrobial materials. *Evid-Based Complement Alternat Med*. 2015;2015(246012):1-16.
4. Rezaie AB, Montazer M, Rad MM. Environmentally friendly low cost approach for nano copper oxide functionalization of cotton designed for antibacterial and photocatalytic applications. *J Cleaner Prod*. 2018;204:425-436.
5. Farig A, Khan T, Yasmin A. Microbial synthesis of nanoparticles and their potential applications in biomedicine. *J Appl Biomed*. 2017;15(4):241-248.
6. Khan A, Rashid A, Younas R, Chong R. A chemical reduction approach to the synthesis of copper nanoparticles. *Int Nano Lett*. 2016;6(1):21-26.
7. Raghunath A, Perumal E. Metal oxide nanoparticles as antimicrobial agents: a promise for the future. *Int J Antimicrob Agents*. 2017;49(2):137-152.
8. Choudhury P, Mondal P, Majumdar S, Saha S, Sahoo GC. Preparation of ceramic ultrafiltration membrane using green synthesized CuO nanoparticles for chromium (VI) removal and optimization by response surface methodology. *J Cleaner Prod*. 2018;203:511-520.
9. Ren G, Hu D, Cheng EWC, Vargas-Reus MA, Reipd P, Allaker RP. Characterisation of copper oxide nanoparticles for antimicrobial applications. *Int J Antimicrob Agents*. 2009;33(6):587-590.
10. Chalandar HE, Ghorbani HR, Attar H, Alavi SA. Antifungal effect of copper and copper oxide nanoparticles against Penicillium on orange fruit. *Biosci Biotechnol Res Asia*. 2017;1(1): 279-284.
11. Joonas E, Arouja V, Olli K, Kahru A.Environmental safety data on CuO and TiO_2 nanoparticles for multiple algal species in natural water: filling the data gaps for risk assessment. *Sci Total Environ*. 2019;647:973-980.
12. Mohanraj R.Antimicrobial activities of metallic and metal oxide nanoparticles from plant extracts. In: Grumezescu AM, ed. *Antimicrobial Nanoarchitectonics*. Romania: Elsevier; 2017.
13. Taran M, Rad M, Alavi M. Antibacterial activity of copper oxide (CuO) nanoparticles biosynthesized by *Bacillus sp.* FU4: optimization of experiment design. *Pharm Sci*. 2017;23(3):198-206.
14. Muwaffak Z, Goyanes A, Clark V, Basit AW, Hilton ST, Gaisford S. Patient-specific 3D scanned and 3D printed antimicrobial polycaprolactone wound dressings. *Int J Pharm*. 2017;527(1-2): 161-170.
15. Botes M, Cloete TE. The potential of nanofibers and nanobiocides in water purification. *Crit Rev Microbiol*. 2010;36(1):68-81.
16. Garibay-Alvarado JA, Espinoza-Cristóbal LF, Reyes-López SY. Fibrous silica-hydroxyapatite composite by electrospinning. *Int J Res Granthaalayah*. 2017;5(2):39-47.
17. Ulery BD, Nair LS, Laurencin CT. Biomedical applications of biodegradable polymers. *J Polym Sci Part B Polym Phys*. 2012; 49(12):832-864.
18. López-Esparza J, Espinoza-Cristóbal LF, Donohue-Cornejo A, Reyes-López SY. Antimicrobial activity of silver nanoparticles in polycaprolactone nanofibers against gram-positive and gram-negative bacteria. *Ind Eng Chem Res*. 2016;55(49): 12532-12538.
19. Taghavi Fardood S, Ramazani A. Green synthesis and characterization of copper oxide nanoparticles using coffee powder extract. *J Nanostruct*. 2016;6(2):167-171.
20. Varughese G, Rini V, Suraj SP, Usha KT. Characterisation and optical studies of copper oxide nanostructures doped with lanthanum ions. *Adv Mat Sci*. 2014;14(4):49-60.
21. Caballero-Briones F Semiconducting thin films prepared by electrochemical modulation for technological devices [PhD thesis]. Barcelona, Spain: Universidad de Barcelona; 2009.
22. Aliah NN, Ansari MN. Thermal analysis on characterization of polycaprolactone (PCL)—chitosan scaffold for tissue engineering. *Int J Sci Res Eng Technol.* 2017;6(2):76-80.
23. Paraguay-Delgado F, Gomez MM, Bianchi AE, et al. Nanopartículas de CuO y su propiedad antimicrobiana en cepas intrahospitalarias. *Rev Colomb Quim*. 2017;46 (3):28-36.
24. Ahamed M, Alhadlaq HA, Khan MA, Karuppiah P, Al-Dhabi NA. Synthesis, characterization, and antimicrobial activity of copper oxide nanoparticles. *J Nanomater*. 2014;2014:637858.
25. Singh A, Dubey AK. Various biomaterials and techniques for improving antibacterial response. *ACS Appl Bio Mater*. 2018; 1(1):3-20.